Cell Reports, Volume *35*

Supplemental information

Reliance on *Cox10* and oxidative metabolism for antigen-specific NK cell expansion

Annelise Y. Mah-Som, Molly P. Keppel, Joshua M. Tobin, Ana Kolicheski, Nermina Saucier, Veronika Sexl, Anthony R. French, Julia A. Wagner, Todd A. Fehniger, and Megan A. Cooper

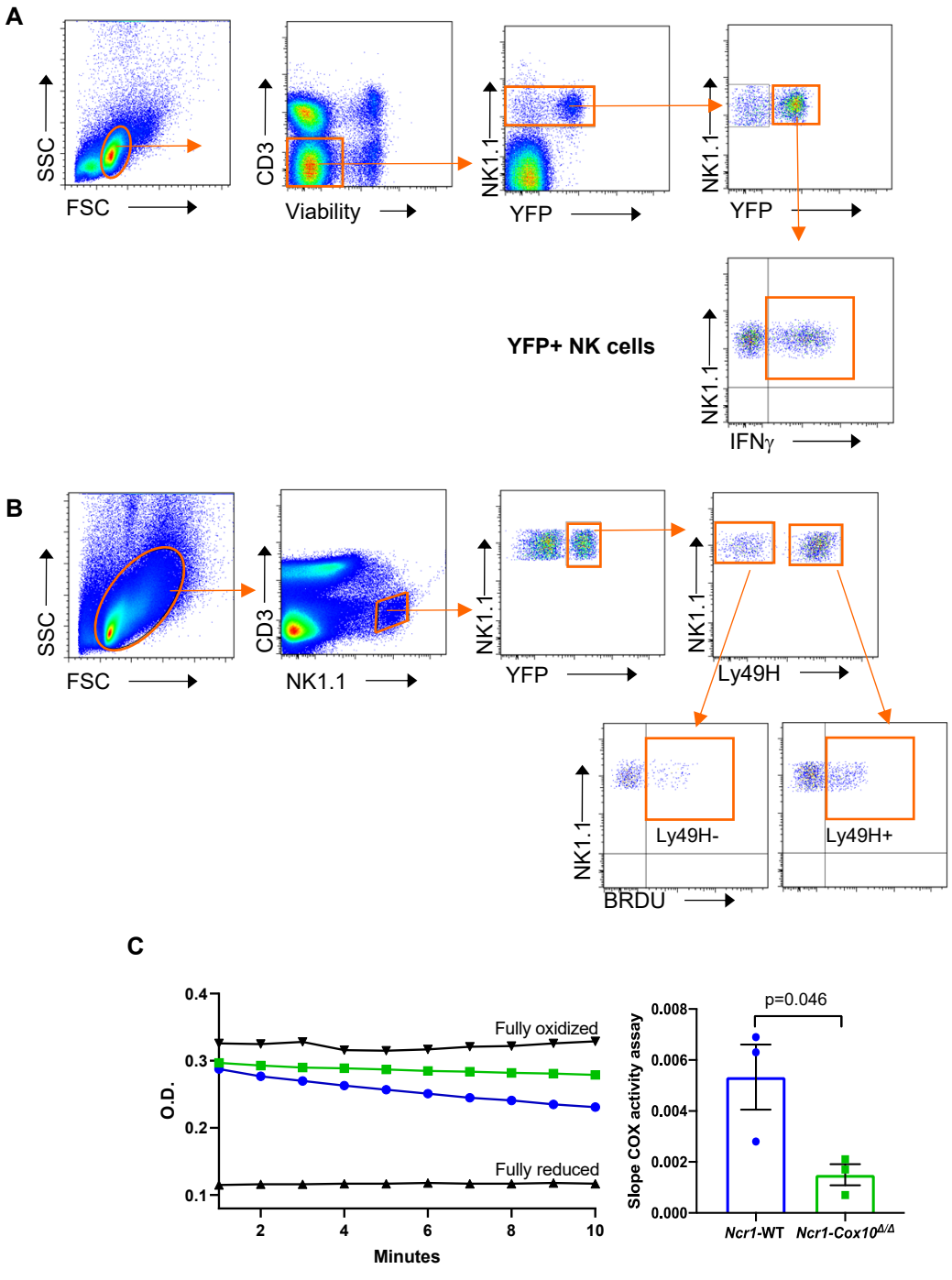

Supplemental Figure 1. Sample flow gating for experiments and Cox activity, related to Figure 1. Sample flow gates shown for *Ncr1-WT* samples. A) Stimulation of splenocytes with cytokines to determine percentage of YFP+ NK cells producing IFNγ, gating on: lymphocytes by FSC/SSC → CD3 negative viable cells → NK1.1 positive cells → YFP+NK1.1+ cells → NK1.1 x IFNγ. B) Analysis of BRDU following MCMV infection (day 4) to determine percentage of YFP+ Ly49H+ or Ly49H- cells that were BRDU-positive, gating on: lymphocytes by FSC/SSC → CD3 negative and NK1.1 positive → NK1.1 and YFP positive cells → NK1.1+ Ly49H negative or positive cells → NK1.1 x BRDU. C) COX activity of FACS-purified YFP^{+} NK cells, COX activity slopes from *Ncr1*-WT and *Ncr1-Cox10*$^{\Delta/\Delta}$ groups (unpaired two-tailed t-test, data shown from 2 separate experiments).

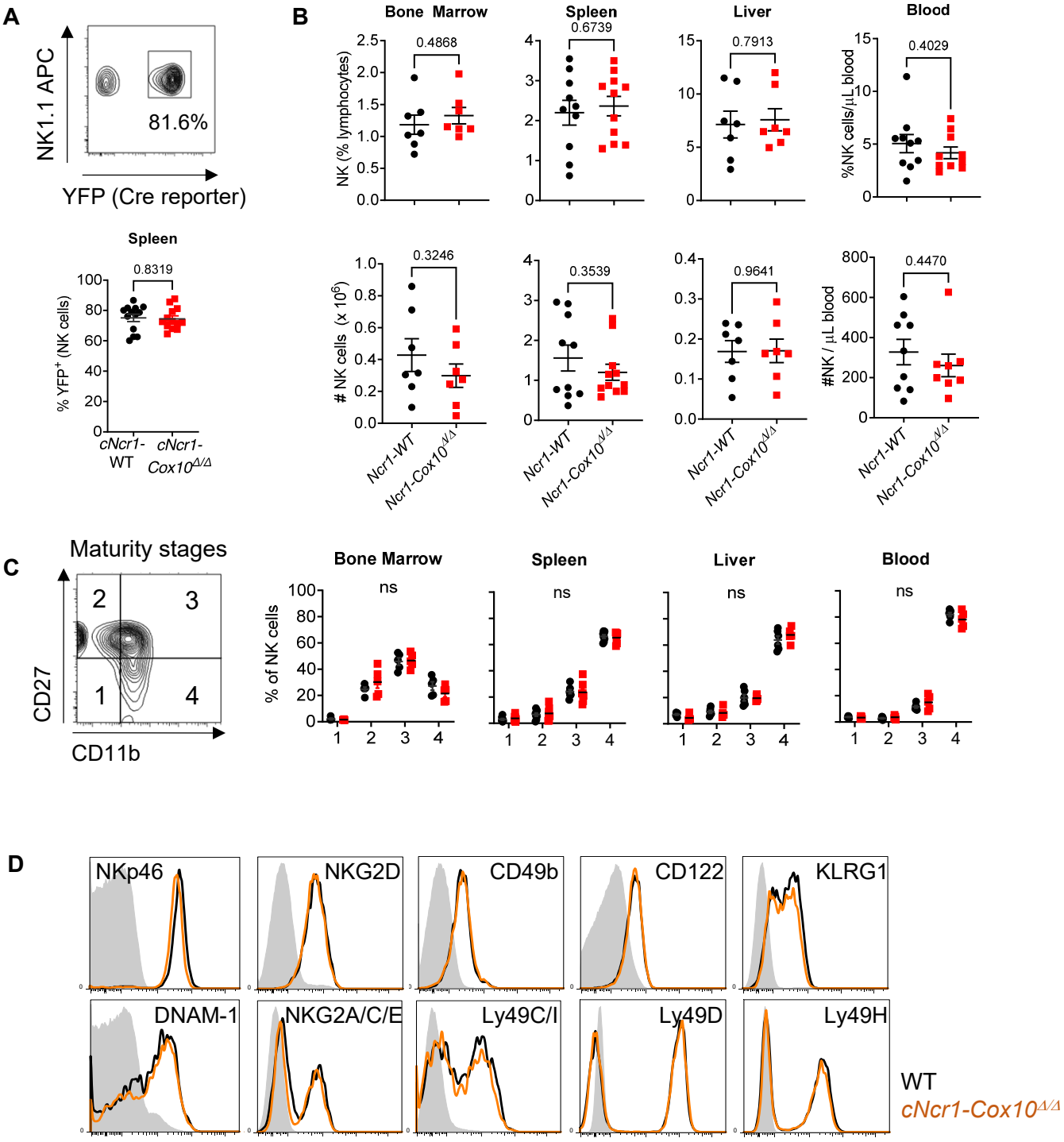

Supplemental Figure 2. NK cell phenotype of *cNcr1-Cox10*$^{\Delta/\Delta}$ mice, related to Figures 1 and 2. NK-specific (*Ncr1*) transgenic Cre mice (Eckelhart et al., 2011) were crossed to YFP reporter and *Cox10*$^{\Delta/\Delta}$ mice to produce constitutive NK-specific *Cox10* deficiency (*cNcr1-Cox10*$^{\Delta/\Delta}$). Mice were compared to *cNcr1*-WT reporter mice. A) Representative flow shows gating on CD3$^-$NK1.1$^+$YFP$^+$ cells and equivalent induction of YFP in splenic cells (n=13/group, 6 separate experiments, unpaired t-test). B) There were similar numbers of YFP+ NK cells in different organs, n=7-10 mice/group in 4 experiments (unpaired t-test). C) NK maturation (of YFP+ NK cells) assessed by CD11b x CD27 was similar, black circles=WT, red squares=*cNcr1-Cox10*$^{\Delta/\Delta}$ (n=5-8/group, 2 separate experiments, analyzed by two-way ANOVA, all comparisons $p<0.05$). D) Representative flow histograms of NK cell receptors on CD3$^-$NK1.1$^+$YFP$^+$ splenocytes from WT (black) and *cNcr1-Cox10*$^{\Delta/\Delta}$ (orange) mice.

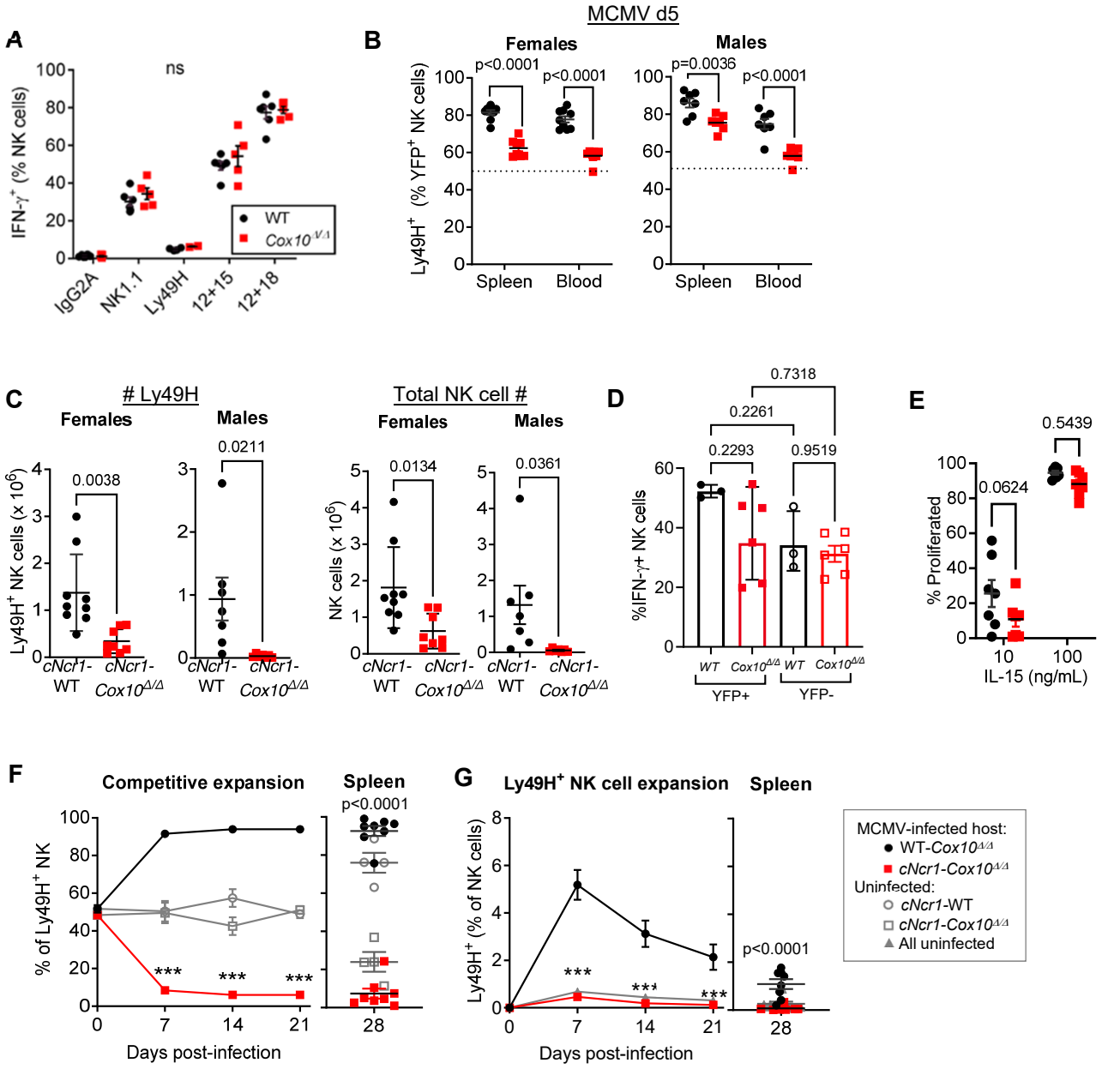

Supplemental Figure 3. Functional testing of *cNcr1-Cox10$^{\Delta/\Delta}$* mice demonstrate impaired Ly49H-driven proliferation with MCMV infection, related to Figures 2 and 4. A) Similar production of IFN-γ by YFP+ *cNcr1-Cox10$^{\Delta/\Delta}$* NK cells compared to control after 6 hours activation via plate-bound receptor antibodies and cytokine stimulation in vitro. n=3-5/group (no significant differences by two-way ANOVA, comparisons between WT and *Cox10* mice were p<0.05). B-C) Mice were infected with MCMV and on day 5 the percentage of Ly49H+ cells among YFP+ cells (Cre-induced) was lower in the spleen and blood of *cNcr1-Cox10$^{\Delta/\Delta}$* compared to controls. C) The number of Ly49H$^+$ NK cells and total NK cells per spleen was decreased in *cNcr1-Cox10$^{\Delta/\Delta}$* mice. For B & C, n=8-9 individuals/group, 2 separate experiments for females (5e4 PFU MCMV), and n=7/group, 2 separate experiments for males (at 7.5e4 and 1.25e5 PFU) with pooled data shown. B analyzed by two-way ANOVA and C by unpaired t-test. D) Similar levels of IFN-γ positive NK cells 1.5 days post-MCMV infection, n=3 mice/group in 2 experiments (two-way ANOVA, pooled data). E) Proliferation to IL-15 was similar between the two models. Splenocytes from Ncr1-YFP reporter (WT) and *cNcr1-Cox10$^{\Delta/\Delta}$* mice were labeled with cell trace violet and cultured in IL-15 at 10ng/mL or 100ng/mL for 5 days, percent proliferation shown (individual mice from pooled experiments, two-way ANOVA). F&G) *cNcr1*-WT and *cNcr1-Cox10$^{\Delta/\Delta}$* NK cells were co-transferred into Ly49H-deficient B6.Bxd8 mice and assessed weekly for expansion of Ly49H+ cells. F) Ratio of WT to *Cox10*-deficient NK cells. G) Percentage of all NK cells that were Ly49H+ (of host origin). (n=5-8 mice/group in 3 separate experiments. Two-way ANOVA with Sidak's multiple comparisons test for days 0-21, one-way ANOVAs with Tukey's multiple comparisons test were used to compare all groups in the spleen at day 28). *** p<0.0001. Graphed are means +/- SEM; error bars too small to be shown are present.

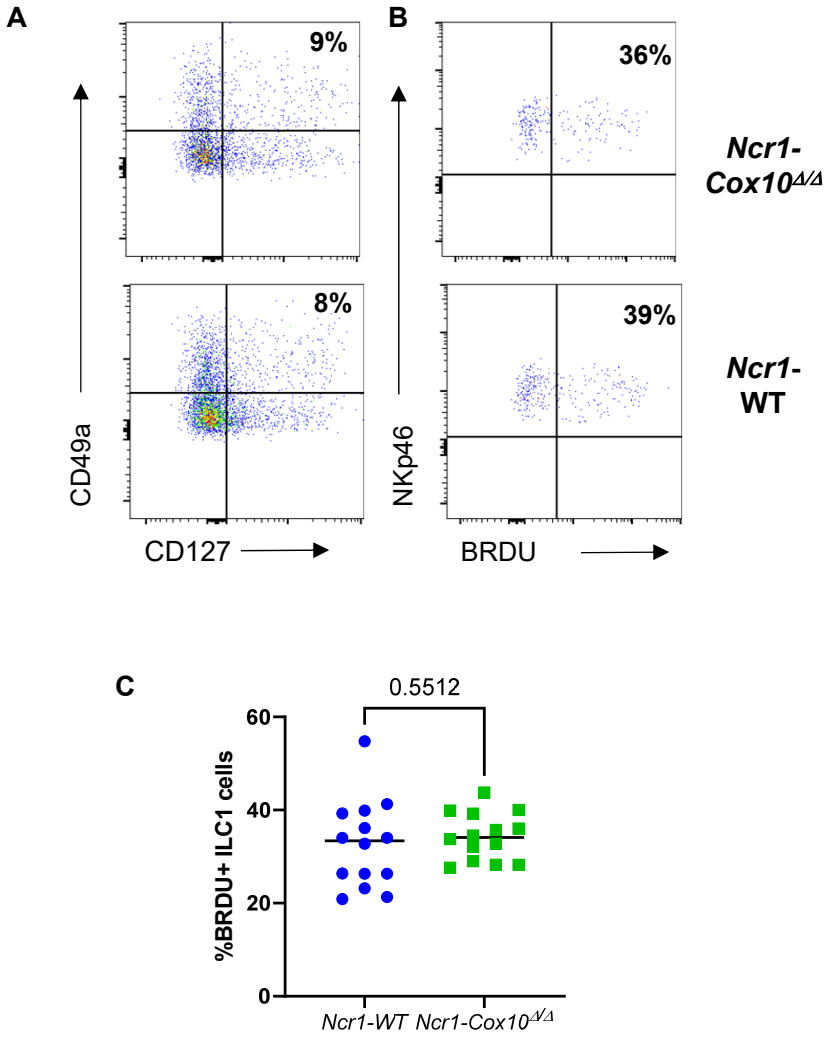

Supplemental Figure 4. ILC1 proliferation in *Ncr1-Cox10*$^{\Delta/\Delta}$ mice is similar to *Ncr1*-WT during MCMV, related to Figure 2. ILC1s were identified in the spleen on day 4 after MCMV infection by first gating on CD45^{+}DX5^{+}NKp46^{+} and Lin-negative (CD3/CD19/CD11c) cells (see Figure 3 for MCMV infection). A) Cells were gated on YFP+ and ILC1 cells identified as CD127^{+}/CD49a^{+}. B & C) YFP+ ILC1s from WT and Cox10-deficient NK cells had similar BRDU incorporation. N=14 WT and 15 Cox10-deficient from 4 separate experiments, student's unpaired t test.

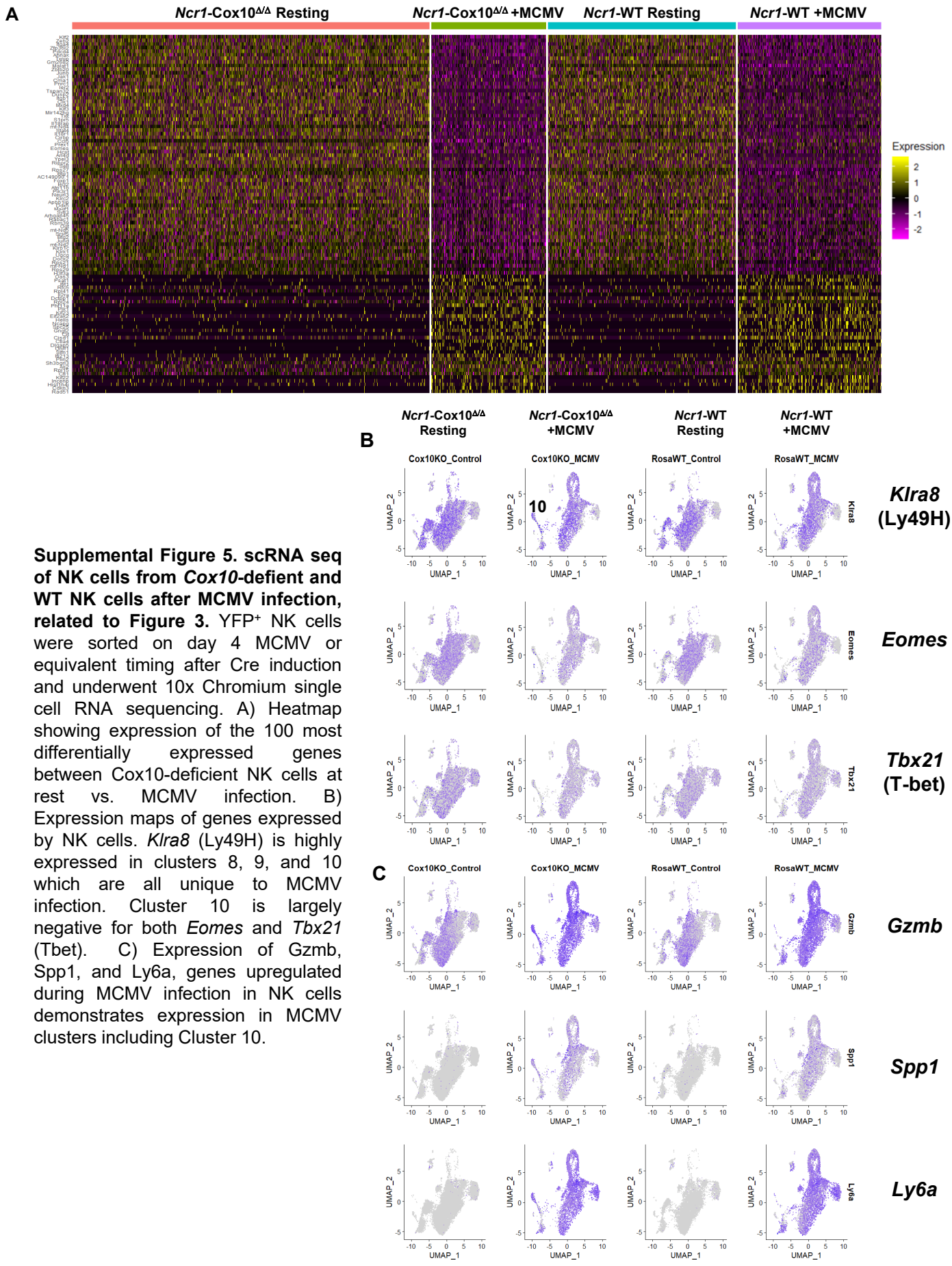

Supplemental Figure 5. scRNA seq of NK cells from *Cox10*-defient and WT NK cells after MCMV infection, related to Figure 3. YFP⁺ NK cells were sorted on day 4 MCMV or equivalent timing after Cre induction and underwent 10x Chromium single cell RNA sequencing. A) Heatmap showing expression of the 100 most differentially expressed genes between Cox10-deficient NK cells at rest vs. MCMV infection. B) Expression maps of genes expressed by NK cells. *Klra8* (Ly49H) is highly expressed in clusters 8, 9, and 10 which are all unique to MCMV infection. Cluster 10 is largely negative for both *Eomes* and *Tbx21* (Tbet). C) Expression of Gzmb, Spp1, and Ly6a, genes upregulated during MCMV infection in NK cells demonstrates expression in MCMV clusters including Cluster 10.

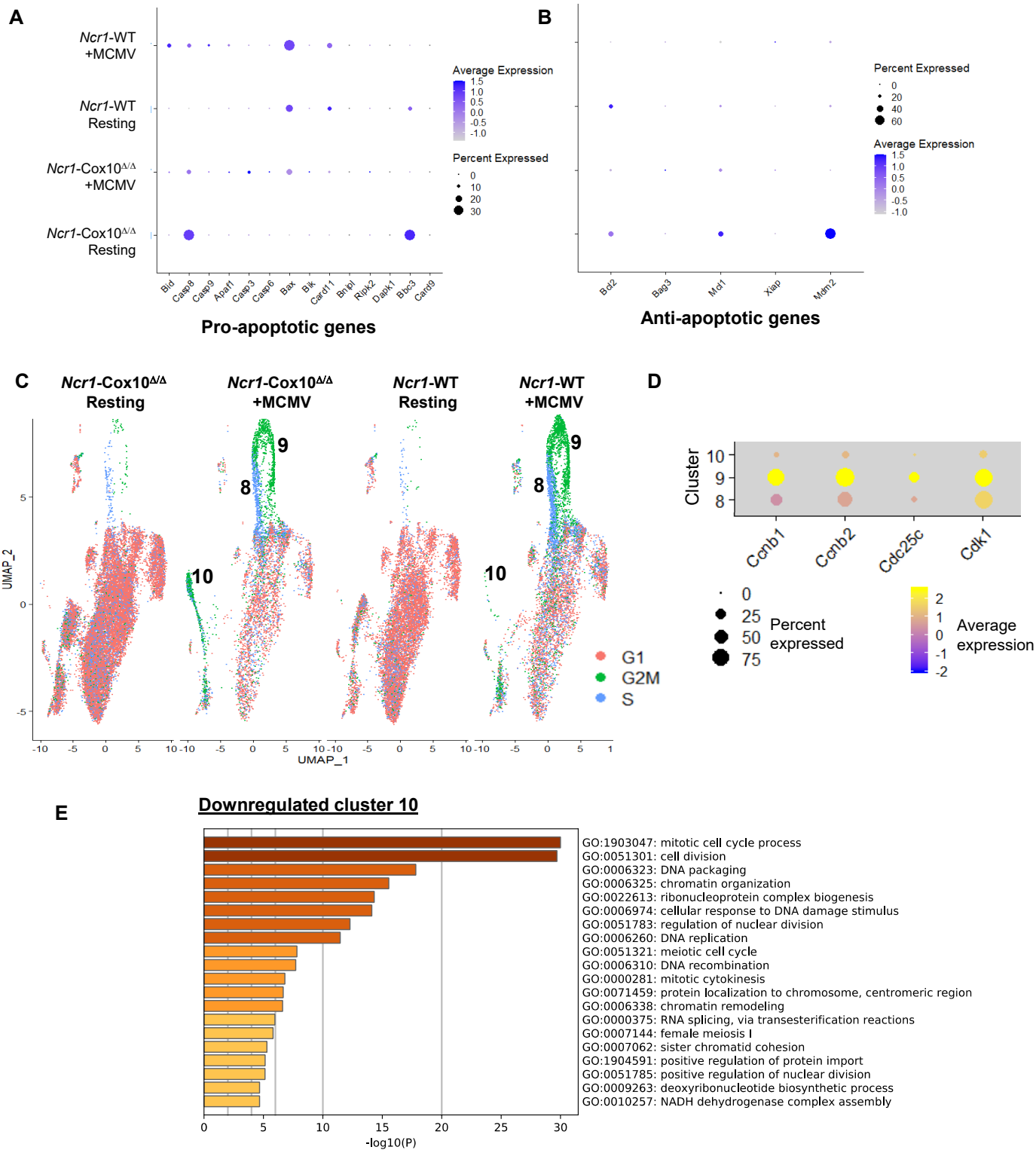

Supplemental Figure 6. Apoptosis, cell cycle analysis, and differentially expressed pathways of NK cells in Cluster 10 unique to *Cox10*-deficient NK cells, related to Figure 3. A&B) Dot plots showing percent of cells per sample expressing gene of interest (size) and average expression of gene (color) of A) pro- and B) anti-apoptotic genes in cluster 10 NK cells. C) Cell cycle analysis (CellCycleScoring, Seurat) of NK cells classified by expression of G1, S or G2/M-related genes. D) Expression of four pro-mitotic cell cycle genes in MCMV-responsive clusters 8, 9, and 10. Average expression level (normalized log fold-change) for each cluster. D) Genes that were significantly downregulated in Cluster 10, MCMV-induced cluster in *Ncr1-Cox10*$^{\Delta/\Delta}$ NK cells. Differentially expressed genes (>0.25 log fold change, adjusted p<0.05) were analyzed for enrichment of GO biological process terms using Metascape; top 20 most significant results shown. Adjusted p value was calculated using Wilcoxon rank sum test with Bonferroni correction.